A Self-Consistent Full 3-D Real-Space NEGF Simulator for Studying Nonperturbative Effects in Nano-MOSFETs

Antonio Martinez, Marc Bescond, John R. Barker, Alexei Svizhenko, M. P. Anantram, Campbell Millar, and Asen Asenov, *Senior Member, IEEE*

***Abstract*—In this paper, we present a full 3-D real-space quantum-transport simulator based on the Green's function formalism developed to study nonperturbative effects in ballistic nanotransistors. The nonequilibrium Green function (NEGF) equations in the effective mass approximation are discretized using the control-volume approach and solved self-consistently with the Poisson equation in order to obtain the electron and current densities. An efficient recursive algorithm is used in order to avoid the computation of the full Green function matrix. This algorithm, and the parallelization scheme used for the energy cycle, allow us to compute very efficiently the current–voltage characteristic without the simplifying assumptions often used in other quantum-transport simulations. We have applied our simulator to study the effect of surface roughness and stray charge on the I_D–V_G characteristic of a 6-nm Si-nanowire transistor. The results highlight the distinctly 3-D character of the electron transport, which cannot be accurately captured by using 1-D and 2-D NEGF simulations, or 3-D mode-space approximations.**

***Index Terms*—Nanowire MOSFET, Nonequilibrium Green Function (NEGF), stray charges, surface roughness.**

I. Introduction

THERE are concerns that atomic-scale inhomogeneities, such as surface roughness, stray dopants, and trapped charges will introduce intolerable variability and degrade the nanoscale CMOS device performance [1]. The quantum-transport simulation of such effects requires full 3-D treatment. This is particularly important in nanowire MOSFETs [2]–[4], which, due to superior transport properties and electrostatic integrity, are becoming strong candidates for nano-CMOS applications near and beyond the end of the current ITRS edition [5].

Three-dimensional quantum-transport simulation studies of atomic-scale variability in nanowire transistors have been initially conducted using a so-called mode-space (MS) approximation [6], which couples 1-D nonequilibrium Green function (NEGF) transport simulations to transverse states obtained from solutions of the Schrödinger equation in 2-D slices. However, the use of the MS method cannot be justified in the case of cross-sectional variation and meandering flows. The coupled-mode (CM) approach [7]–[9], which is a refinement of the MS approach, coupling the different modes between the different cross sections, usually samples a small number of modes to reduce computational complexity [9]. In [9], it has been rigorously applied to simplified 2-D model problems with arbitrary changing cross sections reproducing the results of full 2-D NEGF simulations. Still, its accuracy is questionable in the case of sharp changes in the direction of the current flow, and it has not been tested in the 3-D case in comparison with full 3-D NEGF simulations. *A fortiori*, the present CM formulations cannot handle tunnelling through the oxide regions or gate leakage. Alternatively, the contact-block-reduction approach [10], which reduces the 3-D open-boundary transport problem to a closed-boundary problem, is efficient only when a small number of eigenvectors, and the corresponding eigenvalues, are utilized. The NEGF does not have the above limitations and is ideally suited to 3-D simulations of nanoscale devices with a complex geometry.

In this paper, for the first time, we demonstrate a real-space fully 3-D NEGF formalism coupled self-consistently with the 3-D Poisson equation in order to determine the performances of small nanowire transistors in an efficient way: i.e., by employing an effective mass approximation. This paper extends our previous non self-consistent 3-D NEGF simulation results reported in [11] and [12].

The advantages of the 3-D real-space Green functions are that, even if the potential distributions have discontinuities, the Green functions and their spatial derivatives for each energy will be continuous. Crucially, this leads to the guaranteeing of microscopic current continuity for each electron. Other methods, such as mode decomposition or the MS approach, do not guarantee explicit current continuity at the microscopic level, unless all modes are taken into account. It follows that, when strong discontinuities in the potential occur, the mode- and/or eigenvalue-decomposition methods need to be carefully validated against full methods (that solve the full 3-D problem without projection to lower dimensions and without arbitrary smoothness assumptions).

In this paper, we use anisotropic bulk effective masses rather than confined-geometry masses. Therefore, we do not claim to

Manuscript received January 2, 2007; revised June 1, 2007. The review of this paper was arranged by Editor M. Giles.

A. Martinez, J. R. Barker, C. Millar, and A. Asenov are with the Department of Electronics and Electrical Engineering, University of Glasgow, G12 8LT Glasgow, U.K.

M. Bescond is with L'Institut de Microélectronique, Électromagnétisme et Photonique (IMEP), Institut National Polytechnique de Grenoble (INP)-MINATEC, F-38016 Grenoble Cedex 1, France.

A. Svizhenko is with SILVACO International, Santa Clara, CA 95054, USA.

M. P. Anantram is with the Electrical and Computer Engineering Department, University of Waterloo, Waterloo, ON N2L 3G1, Canada.

Color versions of one or more of the figures in this paper are available online at http://ieeexplore.ieee.org.

Digital Object Identifier 10.1109/TED.2007.902867

0018-9383/$25.00 © 2007 IEEE

Authorized licensed use limited to: University of Washington Libraries. Downloaded on September 13,2024 at 22:03:16 UTC from IEEE Xplore. Restrictions apply.

give a fully quantitative assessment of the quantum transport; instead, we aim to provide a first qualitative insight into the quantum-transport processes; it is nevertheless a reasonable quantitative approximation, as discussed further in Section II.

The capabilities of the simulator are illustrated in the simulation of ballistic transport in a 6-nm channel-length nanowire MOSFET. In this range, the devices are expected to have a high degree of ballisticity, according to recent theoretical studies based on a simplified treatment of inelastic scattering computed by an MS-based Green function method [13], [14]. We have studied the effect of surface roughness and unintentional random dopants on the current–voltage (I–V) characteristics of the nanowire transistor. Our objective is an evaluation of the effect of surface roughness and long-range effects produced by the Coulomb tails of individual unintentional random dopants located in the channel on the I–V characteristics of the nanowire transistor.

In Section II, we provide a deeper discussion of the simulation strategy and the physical model. In Section III, we present the implemented 3-D NEGF formalism. Section IV details technical aspects of the simulator design. The example simulations of a nanowire transistor in the presence of surface roughness and stray charges are presented in Section V, and the conclusions are drawn in Section VI.

II. Computational Strategy and Physical Model

We do not intend a rigorous quantitative study at this stage; however, a qualitative study of different local quantum phenomena due to roughness and unintentional defects in the channel is presented. The capability of the (3-D real space) NEGF simulator to treat these space inhomogeneities and their effect on device performance is the main subject of this paper. At the core of our approach is the assumption of an anisotropic effective mass model for the carriers. In addition, the bulk effective masses have been used in this paper rather than geometry-dependent confined masses. Following the tight-binding (TB) community, the bulk masses are quite similar to the confined masses when the body thickness is larger than 3 nm [15]. Additionally, first-principles analysis for a slab of silicon [16], [17] shows smaller changes in the extracted effective masses due to confinement than that predicted by the TB approach; the changes depend on the assumed atomic structure for the interfaces which is still controversial. Besides, the penetration of the electron-wave function into the oxide increases the effective physical cross section.

It has been argued previously [18] that effective mass theory cannot be used below the 3–4-nm limit without some modifications; however, it is still possible to use the effective mass approximation by calculating the band structure for each nanowire cross section and extracting the new longitudinal and transversal masses. It should be mentioned that, as long as the perturbation coming from roughness leads to small mass changes, the "body-thickness-dependent effective mass" for silicon can still be used down to 1.5-nm body thickness (private communication with K. Nehari, F. Michelini, N. Cavassilas, and M. Lannoo). At that scale (1.5 nm), the energy levels of the three first subbands of the conduction band (the ones which are involved in the electron transport) are exactly the same as the levels resulting from TB calculations. It will then give very similar transmission profiles. It should be observed that our simulation methodology is targeted on devices down to 5-nm body thickness (as the maximum cross section that can be treated), but to speed-up the simulation time, we present results for smaller devices.

The surface roughness is modeled using a randomly generated surface with one interatomic-layer step normal to the interface and an appropriate correlation length. The approach follows our earlier model described in [19] and [20] based on results reported in [21]. The details are given in Section IV, but some general remarks are made here. Ideally, it might be imagined that a full microscopic (atomic level) description of the $Si:SiO_2$ interface would be necessary rather than our phenomenological model. However, the atomic SiO_2 interface is mostly amorphous and difficult to describe precisely; for example, a recent first-principles calculation of a slab geometry [16] shows different results for the extracted mass depending on the way the interface is described. Our phenomenological model provides, instead, an *exemplar* surface that is chosen to approximate our best typical information on the large range of possible microscopic configurations. As discussed in [19] and [20], our interface model is compatible with atomic-level (step) discretization of the interface profile.

Even if it were true that the precise specific atomic-wave functions and orbitals are necessary for device modeling, it is unfortunately true that, at the present time, there is no precise atomistic description of a SiO_2 interface. It is also the case that the potentials that arise from the bare atomistic interface are, in practice, renormalized by the screening processes induced self-consistently by the conduction electrons. Indeed, the devices under consideration are not single-electron devices: Many electrons are involved, and the corresponding states are mostly open-boundary extended states for which the precise electrostatic environment remains unchanged or only slightly affected by the presence of other electrons.

A rigorous treatment of the self-consistent electrostatic-field distribution has proved very important in previous studies for quantitatively accurate descriptions of the correct performance of the devices; changes in oxide thickness, for example, may produces large changes in the output currents. Devices such as nanotransistors are bounded by two large (essentially classical) reservoirs (the source and drain contacts), and the electrostatic coupling described by Poisson's equation (including coupling to the gate electrode) determines the average electrostatic electric-field profile that is "seen" by each conducting electrons. This means that field-distribution accounts for all the other electrons, dopant atoms, and external fields (gate potential, work function, etc.). It is clear, therefore, that the electrostatic self-consistent field plays a crucial role in the regulation of how much current will pass through these devices.

Most published TB simulation papers describe the interface roughness by hydrogen-terminated ends, which indeed represents an atomistic description of the interface; but the true atomic interface of SiO_2 is very different, and even here, there are widely different competing models of the crystalline interface. Moreover, in most cases, the interface is amorphous.

Authorized licensed use limited to: University of Washington Libraries. Downloaded on September 13,2024 at 22:03:16 UTC from IEEE Xplore. Restrictions apply.

It is worth noting that the Slater–Koster approach uses TB as a fitting technique; therefore, it is not clear whether or not the resulting wavefunctions genuinely represent the interface as it is presented to the conduction electrons. Thus, there are inherent limitations in the microscopic alternatives to our model. Any realistic atomistic description of the interface will need to be found using first-principles density functional techniques, which are much more complex and computationally heavy and which are prohibitive for designing simulation tools for modern device optimization and design. It is for the latter reason that our simulation strategy is to pursue the effective mass model and phenomenological interface models as far as possible.

As a final commentary on the effective mass model used here, we comment on the role of fluctuations in the channel width. There are two main effects: One is that the effective oxide thickness changes locally and affects directly the electrostatic-field distributions. The other is due to quantum effects: For long correlation lengths (as in our example for roughness), an additional confinement occurs (nondissipative shift in energy levels and spatial redistribution of charge) as well as scattering induced by the local change of the potential energy near the interface (a momentum-relaxation process). A change in body thickness of 10% implies, theoretically, that a further mass renormalization will occur, but this correction is estimated to be small as compared with the mass associated with the average cross section and as compared with dominant dynamic effects associated with the perturbation in the electrostatics. We observe that the change in the transversal states depend on the penetration of the wave function into the oxide or, in more refined models (atomistic), on the wave function that the electron will occupy in the interface; as we have mentioned, a discussion of this point is in the literature for the SiO_2 interface. We conclude that there remains scope for using corresponding calibrated masses in a future fully quantitative analysis.

In the device model, we consider the uniform doping in source/drain as a technique for enforcing charge neutrality and the correct electrostatic potential in source and drain; the latter are regarded as an extension of a large (macroscopic, dissipative) reservoir at a fixed Fermi level. In principle, to perform a full analysis of dopants in source and drain, discrete dopants should be considered throughout the entire simulation domain. One of the difficulties with a full discrete-doping model of an extended source and drain is that, in principle, we need to solve a complicated many-body problem. We know from extensive many-body theory, developed in the 1960s, that the renormalized solutions for uniformly doped systems at these very high densities are close to our starting model assumptions. Self-averaging effects (Kohn–Luttinger theorems) and screening ensure this. For strong departures from uniform doping in the source and drain, the charge-concentration model is equivalent to an adiabatic extension of the Kohn–Luttinger models.

III. Three-Dimensional NEGF Formulation

The 3-D real-space Green's function method transforms the double-time dependence in the Schrödinger equation to energy space, and all the modes are implicitly included automatically without approximation. The formalism controls the injected carrier energies, but the modal decomposition does not appear explicitly in the formulation nor do the transversal eigenfunctions of the system. In essence, the NEGF method solves the full Schrödinger equation throughout the volume irrespective of the varying cross section. Within limits set by the convergence criteria and mesh discretization, the NEGF method generates both the exact open-boundary Green function and, most importantly, gives explicit current conservation (a feature missing in some modal-decomposition implementations).

In the framework of ballistic transport, the NEGF equations [22] contain similar physics to the solution of the Schrödinger equation but there are certain advantages, one of which is the fact that NEGF approach yields directly the electron density and current without the need to compute the wave functions of the problem. In the NEGF approach, the transport-boundary conditions are more naturally imposed through self-energies and the generalization to inelastic scattering is more straightforward due to the intrinsic use of self-energies.

The following two matrix equations [22] are in the core of the NEGF formalism:

$$\left(H^0_{ik}(E) + \Sigma^R_{ik}(E)\right) G^R_{kj}(E) = I_{ij} \tag{1}$$

$$G^<_{ij}(E) = G^R_{ik}(E)\Sigma^<_{kl}(E)G^A_{lj}(E) \tag{2}$$

where H_0 is the Hamiltonian representing the kinetic energy and the self-consistent electrostatic potential on one particle, Σ^R is the retarded self-energy matrix of the contact; the indexes number the spatial coordinates. This latter matrix is obtained from the contact Green function, which is calculated as in [23]. G^R_{ij} is the retarded Green function and represents the probability amplitude for an electron to move in space from the point x_i to the point x_j. $G^<$ is the less-than Green function [22], which is directly proportional to the density, and $\Sigma^<$ is the scattering self-energy matrix. In our case, the scattering matrix is just proportional to the electron-distribution function and the self-energy of the source and drain. Equation (1) contains the dynamical information, while (2) controls the statistical mechanical information. In the ballistic case, (2) becomes a formula to compute the density and current. From the electrostatic potential and the Fermi energy in the source and drain, we may compute the interim electron density by using (1) and (2).

IV. Simulation Aspects

In the self-consistent simulation approach, the computed interim electron density from (2) is fed back to the Poisson equation and used to compute the new potential. The process is repeated until the difference between the old and new potentials becomes less that the desired tolerance. In order to take into account the effect associated with the quantum resistance of the nanowire leads, the electrostatic potential in the source and drain are allowed to float, corresponding to Neumann (open) boundary conditions. At the same time, the difference between the Fermi levels at the source and drain contacts must be equal to the applied voltage. This is essentially different from the boundary conditions used in the Poisson equation for drift-diffusion and Monte Carlo simulation of electron transport.

Authorized licensed use limited to: University of Washington Libraries. Downloaded on September 13,2024 at 22:03:16 UTC from IEEE Xplore. Restrictions apply.

The interface-roughness model describes the random interface as a randomly generated surface with one interatomic-layer step (0.28 nm) normal to the interface and mesh-space resolution, separating the Silicon and the SiO_2 and the corresponding values of the dielectric constant. The correlation length of 2 nm along the interface plane used to generate the surface is essentially identical to the one used in Monte Carlo simulations to reproduce the Si/SiO_2 universal mobility curve [24]. A recent finite-element coupled MS (CMS) approach to study quantum transport in the presence of interface roughness in 3-D nanowires [25] uses a correlation length of 0.7 nm, which leads to a physically much rougher model.

A 3-D Cartesian mesh with variable mesh spacing is used to discretize the solution domain. In order to include, in a simple way, interface roughness in the simulations, we have adopted a control-volume discretization [19] approach for both the Poisson and the NEGF equations. Following the interface-roughness generation approach, the complex shape of the $Si-SiO_2$ interface is easily approximated by a collection of nodal planes. Hence, a unique dielectric constant can be assigned to every volume element (brick) of the grid. In this case, the Poisson equation can be easily integrated around a node (control-volume discretization), conserving the electric displacement vector around every node and naturally taking into account the dielectric constants of the eight bricks condensing at the node. Bearing in mind that each of the eight bricks could have two different dielectric constants (Si or SiO_2) each node may have 256 essentially different neighborhood configurations. A finite-difference scheme would need to treat all those different cases, but in the control-volume-discretization scheme, these cases are automatically taken into consideration. The volume-discretization technique permits solution of the integral formulation of Poisson's equation; the method allows the dielectric constants of the neighboring points to appear explicitly in the discretization equation. In the case of finite discretization, if the dielectric constant changes from element to element, we require a different discretization equation as compared with the case of a uniform dielectric constant. The difference arises because the displacement vector must be continuous across the interface between different dielectric media. Thus, we would require different equations depending on the particular combination or arrangement of the dielectric constants of the elements, which meet in a node. The number of different arrangement is very large, but in the volume discretization scheme, the continuity of displacement vector is automatically assured, which results with only one type of equation.

An additional advantage of the volume-control discretization is that it automatically includes the image charge created by the different dielectric constants.

Our discretization scheme can be extended to include off-diagonal derivatives in the Hamiltonian, such as $\partial^2/\partial x \partial y$, to account for transport that is not aligned with the principal axes. However, this will introduce coupling with diagonal points in a rectangular mesh. This leaves the coupling between different cross sections still local (i.e., just the neighboring cross sections are coupled to each other), and therefore, the recursive algorithm can still be used, but now, every element in a cross section is coupled to five elements in the neighboring cross sections. This produces a five-diagonal-block matrix. The introduction of the nondiagonal mass tensor would require simple modifications, but essentially, the block structure of the recursive algorithm will remain the same.

In order to compute the electron and current density, only the diagonal and the first offdiagonal blocks of $G^<$ are needed. The corresponding matrix elements are efficiently calculated using the recursive algorithm described in more details in [22]. It is based on the standard algorithm that is used to compute particular elements of the Green function using the Dyson equation [22] recursively without inverting the whole matrix. The difference as compared to this standard recursive algorithm is associated with the fact that, in our case, the Dyson equation for $G^<$ is more complicated than the usual Dyson equation because of its coupling with G^R. The algorithm exploits the total symmetry of (1) and (2), minimizing the computational time used. The inversion of the full 3-D $N_x \times N_y \times N_z$ matrix is replaced by N_z inversions of $N_x \times N_y$ matrices, where N_z is the number of nodes along the transport direction and N_x and N_y are the number of nodes in the device cross section. Apart from speeding up the computations, the recursive algorithm also reduces the memory footprint of the simulator. As an example, a relatively small mesh $(N_x \times N_y \times N_z)$ $20 \times 20 \times 100$ will produce a 3-D matrix with a 1.6×10^9 elements.

In the NEGF simulation approach, the single-particle energy E is discretized, and (1) and (2) are solved for each discretization energy value E_i. The total electron density and current are calculated by summing the weighted contributions associated with each discrete energy E_i. The accuracy of the results, particularly in the presence of quantization and resonance, depends on the accurate sampling of the relevant energy space. In order to reduce further the computation time, the energy cycle is parallelized using OpenMP, allowing the computation of the density for every energy separately on different processors, which leads to very high parallel efficiency. The typical number of energy cycles is around 400, and by using 30 processors in parallel, the overall computation time is reduced to approximately 3% of the time of the equivalent serial run. Running on 15 processors on a (shared memory) SGI Origin 300 machine with 500-MHz processors takes one day to produce a point on an I–V curve, with 20 Poisson/NEGF iterations to achieve self-consistence. Therefore, we are able to obtain a complete I–V curve in approximately one week.

V. Application to Nanowire MOSFETs

In very small nanowire transistors, surface roughness and discrete defects introduce nonperturbative effects, which greatly distort the transverse wave function from cross section to cross section along the transport direction. Such effects lead to a current-density vector that is not necessarily parallel to the transport direction: The flow direction alters along the channel of the transistor leading to a meandering current flow.

In order to demonstrate the capabilities of our 3-D NEGF simulator, we have simulated a gate-all-around silicon nanowire MOSFET with 2.2×2.2 nm^2 cross section, 6-nm channel length, and 1-nm gate oxide thickness, as illustrated in Fig. 1.

Authorized licensed use limited to: University of Washington Libraries. Downloaded on September 13,2024 at 22:03:16 UTC from IEEE Xplore. Restrictions apply.

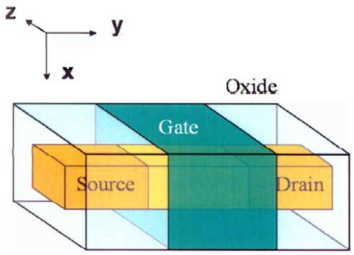


Fig. 1. Nanowire transistor and the orientation of the coordinated system; y is the transport direction.

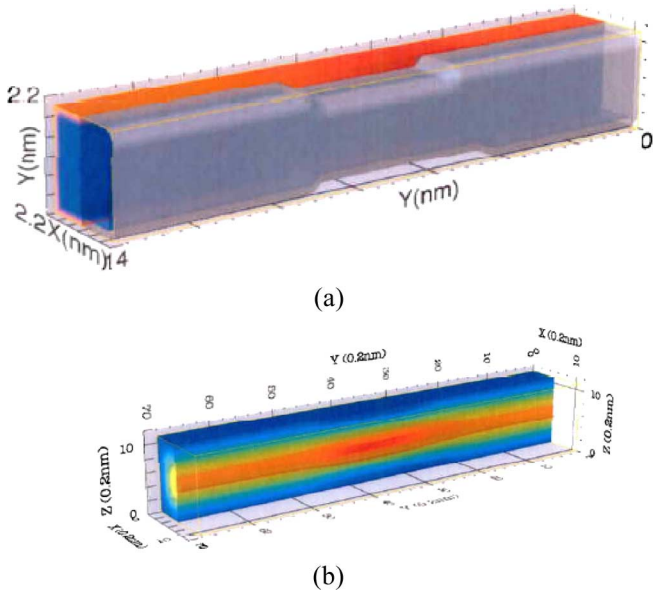


Fig. 2. (a) Three-dimensional view of the rough-surface potential through a constrained nanowire. (b) Three-dimensional view of the current of the constricted nanowire.

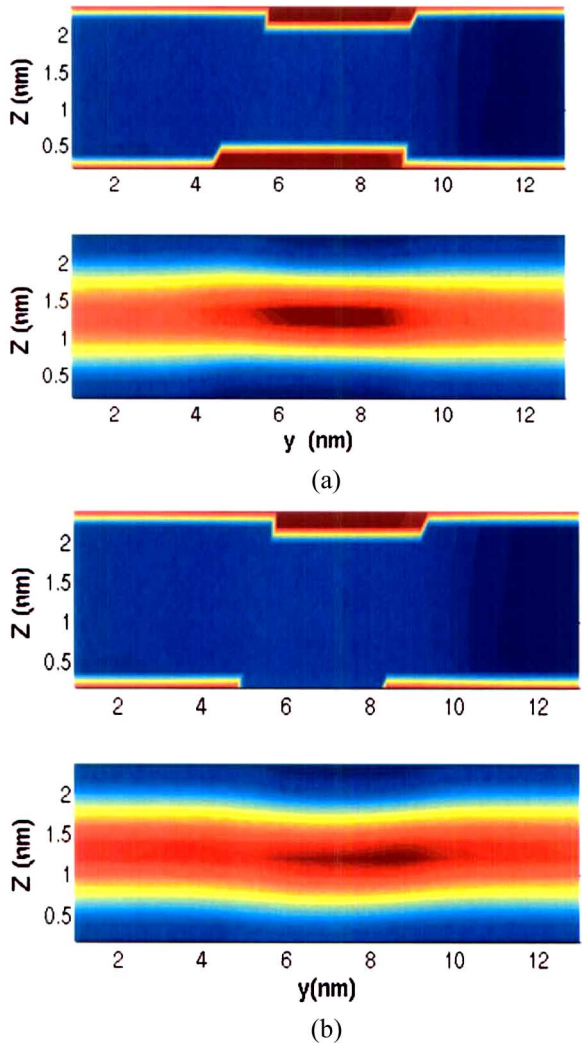


Fig. 3. (a) Nanowire with constriction. Upper: Potential profile. Lower: Current-density profile (both at $x = 1.1$ nm). (b) Potential and current density in a stepped nanowire ($x = 1.1$ nm).

The doping in the source and drain region is 1×10^{20} cm^{-3}, and the channel is undoped. The Poisson equation is solved in the external box of Fig. 1, and the Green function equations are solved in the internal box. As noted in Section II, we use the anisotropic bulk effective masses.

Initially, we focus on the effects associated with the atomic-scale roughness at the channel/gate dielectric interface. In all the simulations of this paper, the surface roughness is only considered in the channel region. Fig. 2(a) shows the 3-D surface potential distribution associated with one randomly generated atomic-scale interface-roughness configuration at $V_G = 0.4$ V and $V_D = 0.2$ V. In this case, the interface roughness produces a constriction in the middle of the channel. Fig. 2(b) shows the 3-D plot of isosurfaces of the y-component of the current density. The tubular isosurfaces became wider in the middle of the channel, reflecting an increase in current density. The color code of the figures associates maximum values of the mapped field to the dark red color and minimum values to the dark blue color.

Fig. 3(a) maps in the zy plane the electrostatic potential and the current density for the constricted nanowire from Fig. 2 at $V_G = 0.4$ V and $V_D = 0.2$ V. The current density increases in the middle of the channel due to the constraint. Fig. 3(b) shows the potential and current in the same plane but for a nanowire with a synchronized step in both the top and bottom interfaces, which does not reduce the cross section but increases the current path. In this case, the current changes direction in the vicinity of the step, following a meandering path.

Fig. 4(a) and (b) shows the electrostatic potential along the middle of the channel, in both the uniform and the constricted devices, respectively, for gate voltages in the range of 0.1–0.5 V and a drain voltage of 0.2 V. The electrostatic potential distribution at low gate bias is similar for both devices. At high gate bias ($V_G = 0.4$–0.5 V), the gate control of the electrostatic potential in the constriction region is stronger, resulting in lower potential compared to the uniform case. It is interesting to compare these results which show a relatively smooth electrostatic potential with the CMS study [25], which shows a very rough variation in electrostatic potential (even in the source and drain regions), and where the CMS study uses a longer channel length, larger cross section, and very much rougher interface-roughness profile. The electron-density distributions along the channel of the uniform and the constricted devices, under the same bias conditions, are illustrated in Fig. 5(a) and (b), respectively. Despite the better electrostatic

Authorized licensed use limited to: University of Washington Libraries. Downloaded on September 13,2024 at 22:03:16 UTC from IEEE Xplore. Restrictions apply.

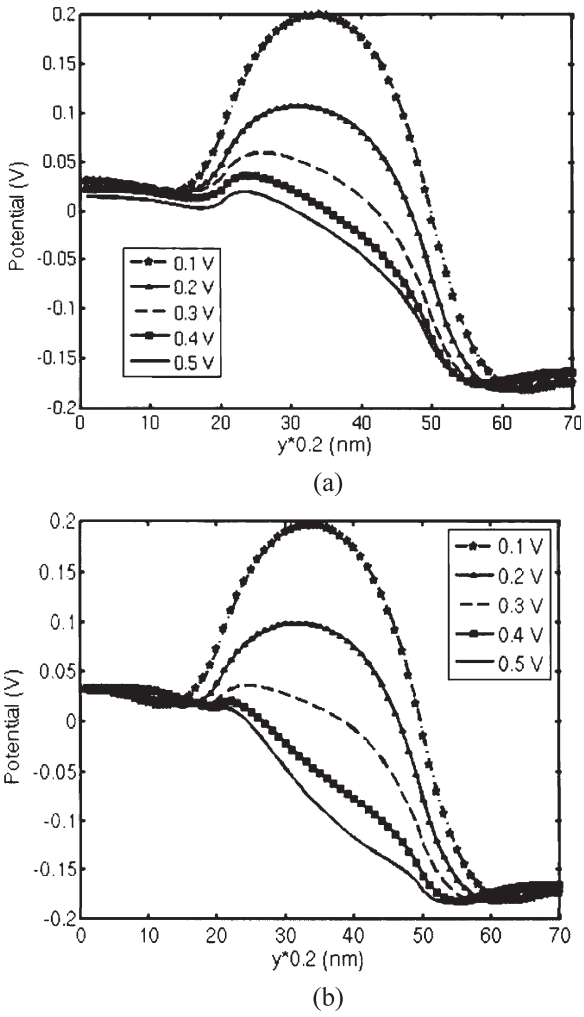


Fig. 4. (a) Potential along the center of the uniform nanowire at different gate biases. (b) Potential along the constricted nanowire for different gate bias.

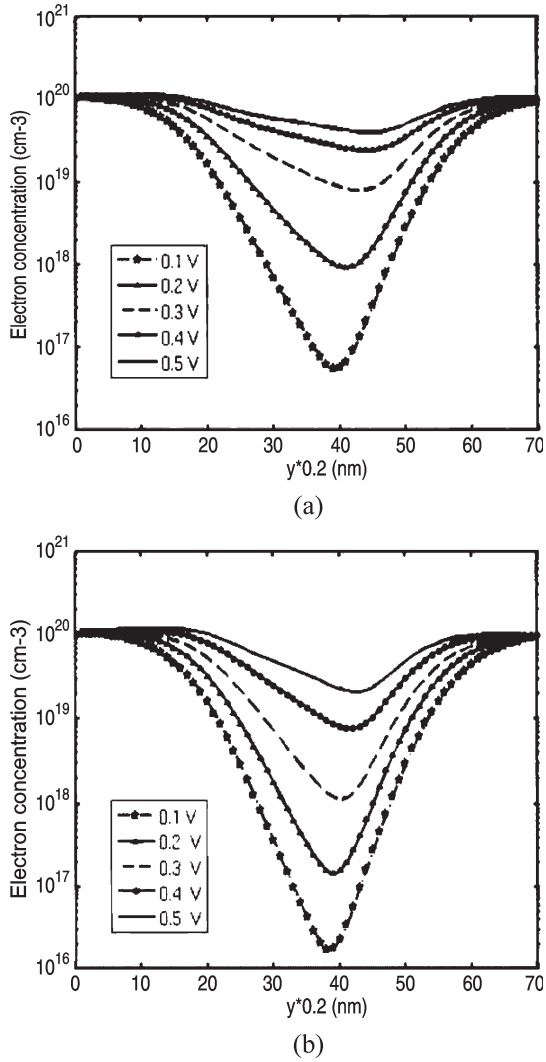


Fig. 5. (a) Electron concentration the along the uniform nanowire. (b) Electron concentration along the constrained nanowire.

control, the electron density in the constrained device at equivalent gate biases is lower as compared to the uniform device. This is due to an energy shift in the transverse states in the constriction. For the same reason, the injection of electrons in the channel of the constrained device is lower when compared to the smooth device at all gate voltages.

The I_D–V_G characteristics of the uniform device and the two devices from Fig. 3 are shown in Fig. 6. The effect of the constriction is dramatic and produces a threshold voltage shift of 150 mV when compared to the uniform device. The threshold voltage shift of the device with synchronised step ($\sim$50 mV) is significantly smaller. Additionally, the ON-current at $V_G =$ 0.5 V in the constrained device is three times smaller than that in the uniform device. The constriction introduces a change in body thickness, which is around 30% of the original thickness. The effect on the carrier concentration and the current is not perturbative, and the corresponding change in current is large. The difference between the I_D–V_G curves of the nanowire with the synchronized steps and the uniform one reflects the effect of the surface-roughness scattering only. Clearly, for the nanowire studied here, the confinement effect has a much greater impact on the current compared with the scattering coming from the interface roughness. However, with the increase in the nanowire cross section, the confinement effects associated with atomic-scale interface roughness will play a less important role.

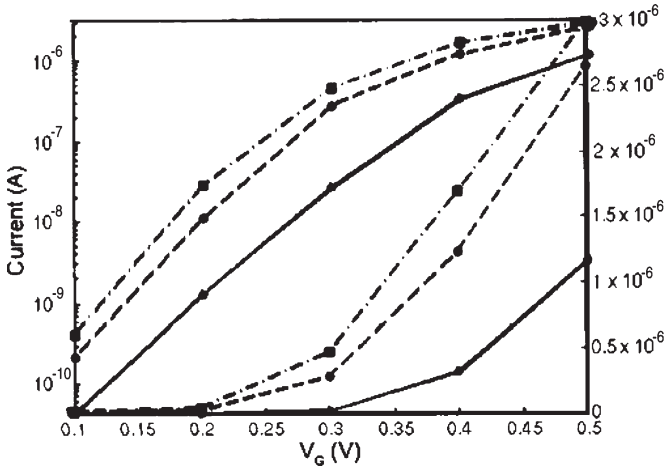


Fig. 6. (dot dash) I_D–V_G characteristics of the uniform nanowire, (dashed) stepped nanowire, and (solid) constrained nanowire.

Authorized licensed use limited to: University of Washington Libraries. Downloaded on September 13,2024 at 22:03:16 UTC from IEEE Xplore. Restrictions apply.

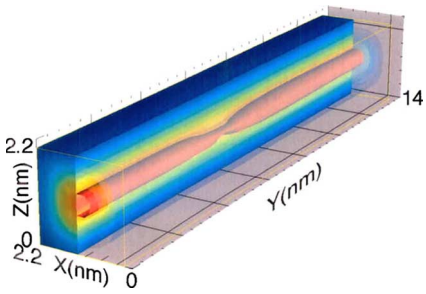


Fig. 7. Three-dimensional plot of the y-current component in a nanowire with a single impurity in the center of the channel.

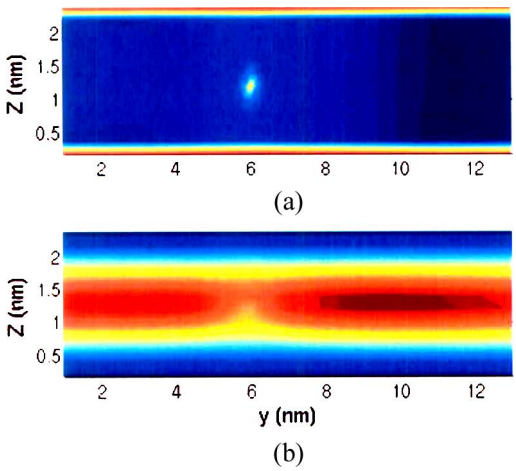


Fig. 8. Potential in a nanowire with an impurity in the (upper) middle of the channel and (lower) current density, at $x = 1.1$ nm.

Fig. 7 shows the isosurfaces of the y-component of the current density in a nanowire with a single electronic charge associated with an ionized acceptor or a trapped electron located almost at the middle of the channel ($x = 1.1$ nm, $y = 6.0$ nm, and $z = 1.1$ nm) $V_G = 0.4$ V and $V_D = 0.2$ V. The electrons are able to propagate across the middle of the channel mainly through the ground state in the potential created by the impurity and the channel interface, which requires higher injection energy. There is also a small contribution associated with a direct tunneling through the Coulomb potential. This is reflected in the narrowing of the tubular isosurfaces at the middle of the channel. The situation is clarified further in Fig. 8(a) and (b),which maps the electrostatic potential and the current density through the impurity in the $z-y$ plane. Note the crowding of the current between the impurity and the interface.

The potential distribution along the center of the channel for different positions of the impurity in the xz plane at $y = 6$ nm and at low gate bias $V_G = 0.2$ V and $V_D = 0.2$ V is illustrated in Fig. 9. Fig. 9 indicates that the potential due to the impurity rises locally to the seemingly large value of 2 eV. This is a consequence of the impossibility of screening the short-range part of the Coulomb potential. Practically, there is no consequence of this large peak for transport. The tunneling in the immediate vicinity of this potential is 99% for thermal electrons, so the quantitative effect of this large energy is negligible for transport. The 2-eV peak is removable if the impurity charge is delocalized more (as would be obtained in a full many-body treatment). However, to do this rigorously requires more detailed knowledge of the wave function to be certain that the distribution of the charge does not affect the long-range Coulomb tail. A better treatment could be performed from density functional methods but they would introduce other complications that hamper the description of transport.

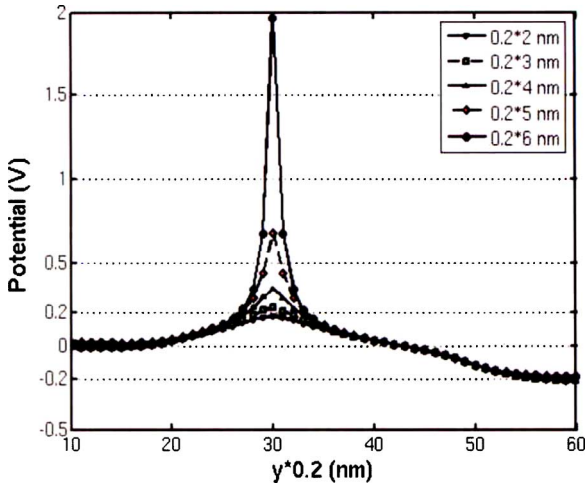


Fig. 9. Potential profile along the channel at different distances from the interface (at low bias).

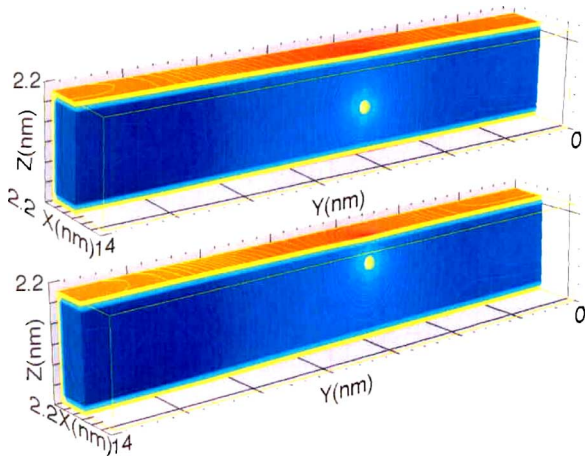


Fig. 10. Potential contour plots for the impurity located at (1.1, 6.0, 1.1) nm and (1.1, 6.0, 1.5) nm.

The impact of the Coulomb tail on the potential barrier in the middle of the channel is still strong even when the impurity is 1 nm off the center of the channel. In order to study the current sensitivity with respect to the position of the impurity in a particular cross section of the channel, we have carried out simulation for two impurity positions ($x = 1.1$ nm and $z = 1.1$ nm) and ($x = 1.1$ nm and $z = 1.5$ nm) in the xz plane at $y = 6$ nm. The isocontours of the electrostatic potential at $V_G = 0.4$ V and $V_D = 0.2$ V are plotted in Fig. 10(a) and (b) for the two impurity configurations. The electrostatic perturbation caused by the impurities in the channel is rather strong for both impurity positions and should have a strong impact on the I_D–V_G characteristic.

Fig. 11 illustrates the isosurface plot of electron concentrations for the impurity in the middle of the channel for low

Authorized licensed use limited to: University of Washington Libraries. Downloaded on September 13,2024 at 22:03:16 UTC from IEEE Xplore. Restrictions apply.

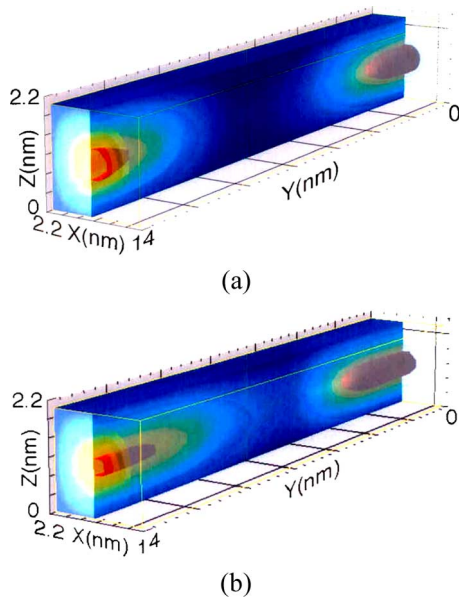


Fig. 11. (a) Electron density isosurfaces at low gate bias with the impurity in the middle of the nanowire. (b) Electron density isosurfaces at high bias with the impurity in the middle of the nanowire.

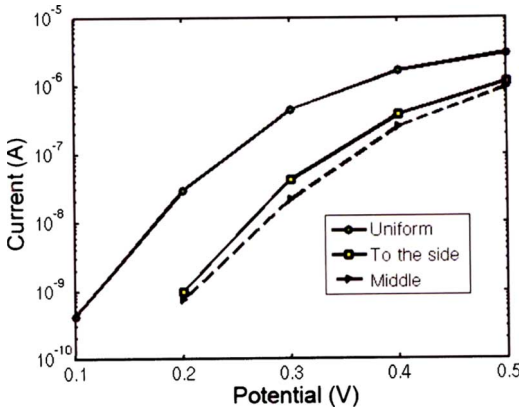


Fig. 12. I_D–V_G characteristics of the uniform and nonuniform nanowires.

($V_G = 0.2$ V) and high ($V_G = 0.4$ V) gate bias. The high-doping regions in the source and drain are clearly seen. At high gate bias, the electron concentration at the source extends farther in the channel as expected. In essence, Fig. 11 shows the effect of the Coulomb tail, which has been screened by the conduction electrons from the drain but which still produces a blocking effect on the electron entering from the source. The isosurface line shows a stronger screening of the impurity potential in the drain side due to the high doping in that region.

Fig. 12 compares the I_D–V_G characteristics of the uniform device, and the two devices with a single negative charge in the middle and 1 nm off the middle of the channel at $y = 6$ nm. The characteristics of the transistors with the two different positions of the impurities are very similar, both yielding a threshold voltage shift of approximately 100 mV. This similarity is associated with the small ($\sim$2.2 nm) cross section of the nanowire, which is comparable with the characteristic radius of the screened Coulomb potential, which is on the order of 1 nm, as shown in Figs. 9 and 10.

VI. Conclusion

We have developed a full 3-D real-space NEGF simulator for the future generation nano-CMOS devices, which can handle nonperturbative effects associated with interface roughness, body-thickness variation, and random discrete dopants. The simulator is parallelized in respect of the energy cycle and uses an efficient recursive algorithm. The simulator allows full 3-D real-space quantum calculations of small transistor on medium-size SMP platforms.

The capabilities of the simulator have been illustrated in a qualitative study of the effect of interface roughness and stray charges in the channel of a nanowire gate-all-around transistor. The full 3-D NEGF simulations at room temperature produce smooth monotonic I_D–V_G characteristics, despite size-quantization and contributing subband quantum transport. Surface roughness has a dramatic effect at nanoscale dimensions due to the energy shifts, surface-roughness scattering, and 3-D meandering current flows associated with the random surface-roughness configurations. Constrains of the channel have a more dramatic effect on the current compare to synchronised roughness that does not change the channel width. The influence of a single dopant on device behavior is dramatic, independent of its spatial location due to the comparable characteristic Coulomb radius and the cross-sectional dimensions of the nanowire channel.

References

[1] A. Asenov, A. R. Brown, J. H. Davies, S. Kaya, and G. Slavcheva, "Simulation of intrinsic parameter fluctuations in decananometer and nanometer scale MOSFETs," *IEEE Trans. Electron Devices*, vol. 50, no. 9, pp. 1837–1852, Sep. 2003.

[2] J. Goldberger, A. Hochbaum, R. Fan, and P. Yang, "Silicon vertically integrated nanowire field effect transistors," *Nano Lett.*, vol. 6, no. 5, pp. 973–977, May 2006.

[3] J. R. Barker, A. Martinez, A. Svizhenko, A. Anantram, and A. Asenov, "Green function study of quantum transport in ultra-small devices with embedded atomistic cluster," *J. Phys.: Conf. Ser.*, vol. 35, pp. 233–246, 2006.

[4] A. Martinez, A. Svizhenko, M. P. Anantram, J. R. Barker, and A. Asenov, "A NEGF study of the effect of surface roughness on CMOS nanotransistors," *J. Phys.: Conf. Ser.*, vol. 35, pp. 269–274, 2006.

[5] *International Technology Road Map for Semiconductors*. [Online]. Available: http://public.itrs.net/

[6] R. Zen, R. Venugopal, S. Goasguen, S. Datta, and M. S. Lundstrom, "NanoMOS 2.5: A two dimensional simulator for quantum transport in double-gate MOSFETs," *IEEE Trans. Electron Devices*, vol. 50, no. 9, pp. 1914–1925, Sep. 2003.

[7] J. R. Barker, "Theory of quantum transport in lateral nanostructures," in *Nanostructure Physics and Fabrication*, M. Read and W. P. Kirk, Eds. New York: Academic, 1989, pp. 253–262.

[8] J. R. Barker, J. Pepin, M. Finch, and M. Laughton, "Theory of non-linear transport in quantum waveguides," *Solid State Electron.*, vol. 32, no. 12, pp. 1155–1159, Dec. 1989.

[9] M. Luisier, A. Schenk, and W. Fichtner, "Quantum transport in two- and three-dimensional nanoscale transistors: Coupled mode effects in the nonequilibrium Green's function formalism," *J. Appl. Phys.*, vol. 100, no. 4, p. 043713, Aug. 2006.

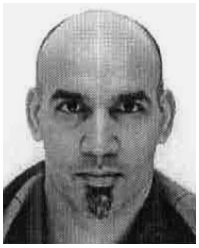
[10] D. Mamaluy, M. Sabathil, and P. Vogl, "Efficient method for the calculation of ballistic quantum transport," *J. Appl. Phys.*, vol. 93, no. 8, pp. 4628–4633, Apr. 2003.

[11] A. Martinez, K. Kalna, J. R. Barker, and A. Asenov, "A study of the interface roughness effect in Si-nanowires using a full 3-D NEGF approach," *Physica E.,* in press.

[12] A. Martinez, J. R. Barker, M. Bescond, A. Svizhenko, M. P. Anantram, and A. Asenov, "Development of a full 3D NEGF nano-CMOS simulator," in *Proc. Int. Conf. Simul. Semicond. Processes and Devices*, 2006, pp. 353–355.

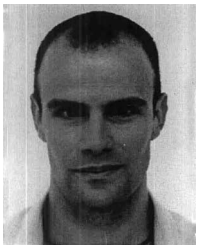
Authorized licensed use limited to: University of Washington Libraries. Downloaded on September 13,2024 at 22:03:16 UTC from IEEE Xplore. Restrictions apply.

[13] S. Jin, Y. J. Park, and H. S. Min, "Influence of electron-phonon interactions on the electronic transport in nanowire transistors," in *Proc. Int. Conf. Simul. Semicond. Processes and Devices*, 2006, pp. 35–38.
[14] S. Jin, Y. J. Park, and H. S. Min, "A three dimensional simulation of quantum transport in silicon nanowire transistor in the presence of electron–phonon interactions," *J. Appl. Phys.*, vol. 99, no. 12, p. 123 719, Jun. 2006.
[15] Y. Zheng, C. Rivas, R. Lake, K. Alam, T. Boykin, and G. Klimeck, "Electronic properties of silicon nanowires," *IEEE Trans. Electron Devices*, vol. 56, no. 6, pp. 1097–1103, Jun. 2005.
[16] Y. Teratani, T. Ando, H. Tsuchiya, and T. Miyoshi, *Extended abstracts of the ICSSDM*, p. 270, 2005, Kobe, Japan.
[17] A. Martinez, K. Kalna, P. Sushko, A. L. Shluger, J. R. Barker, and A. Asenov, in *Proc. Silicon Nanoelectronics Workshop*, Kyoto, Japan, 2007.
[18] J. Wang, A. Rahman, A. Ghosh, G. Klimeck, and M. Lundstrom, "On the validity of the parabolic effective-mass approximation for the I-V calculation of silicon nanowire transistors," *IEEE Trans. Electron Devices*, vol. 52, no. 7, pp. 1589–1595, Jul. 2005.
[19] A. Martinez, A. Svizhenko, M. P. Anantram, J. R. Barker, A. R. Brown, and A. Asenov, "A study of the effect of the interface roughness on a DG-MOSFET using a full 2D NEGF technique," in *IEDM Tech. Dig.*, 2005, pp. 627–630.
[20] A. Asenov, S. Kaya, and J. H. Davies, "Intrinsic threshold voltage fluctuations in decanano MOSFETs due to local oxide thickness variations," *IEEE Trans. Electron Devices*, vol. 49, no. 1, pp. 112–119, Jan. 2002.
[21] S. M. Goodnick, D. K. Ferry, C. W. Wilmsen, Z. Lilienthal, D. Fathy, and O. L. Krivanek, "Surface roughness at the Si(100)-SiO_2 interface," *Phys. Rev. B, Condens. Matter*, vol. 32, no. 12, pp. 8171–8186, Dec. 1985.
[22] A. Svizhenko, M. P. Anantram, T. R. Govindan, B. Siegel, and R. Venugopal, "Two-dimensional quantum mechanical modeling of nanotransistors," *J. Appl. Phys.*, vol. 91, no. 4, pp. 2343–2354, Feb. 2002.
[23] R. Venugopal, Z. Ren, S. Datta, and M. Lundstrom, "Simulating quantum transport in nanoscale transistors: Real versus mode-space approaches," *J. Appl. Phys.*, vol. 92, no. 7, pp. 3730–3739, Oct. 2002.
[24] S. Takagi, A. Toriumi, M. Iwase, and H. Tango, "On the universality of inversion layer mobility in Si MOSFETs: Part I—Effects of substrate impurity concentration," *IEEE Trans. Electron Devices*, vol. 41, no. 12, pp. 2357–2362, Dec. 1994.
[25] J. Wang, E. Pollizi, A. Ghosh, S. Datta, and M. Lundstrom, "Theoretical investigation of surface roughness scattering in silicon nanowire transistors," *Appl. Phys. Lett.*, vol. 87, no. 4, p. 043101, Jul. 2005.



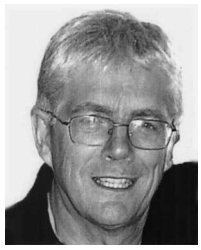
Antonio Martinez received the M.Sc. degree in physics from the University of Havana, Havana, Cuba, in 1987, the M.Sc. degree in physics from the University of Umea, Umea, Sweden, In 1997, and the Ph.D. degree from the Royal Institute of Technology, Stockholm, Sweden, in 2003. His Ph.D. thesis deals with electron transport in anisotropic materials (SiC, GaN) at high electric field using various simulation techniques as drift diffusion, ensemble Monte Carlo, and quantum Monte Carlo.

He is currently a member of the Device Modeling Group with the Department of Electronics and Electrical Engineering, University of Glasgow, Glasgow, U.K. His experiences include Monte Carlo simulation technique for electron and hole transport and nanoscale quantum electron transport using full 3-D nonequilibrium Green's functions approach, specifically simulation of nanoscale MOSFET and nanowire transistors.



Marc Bescond was born in Aubagne, France, in 1978. He received the Master's degree in material engineering from the National Institute of Applied Sciences, Lyon, France, in 2001 and the Ph.D. degree from the University of Provence, Marseille, France, in 2004 (thesis supervisor: M. Lannoo).

He was a Postdoctoral member with the Device Modeling Group of Prof. A. Asenov at the University of Glasgow, Glasgow, U.K. Since 2005, he has been an Associate Professor of electrical engineering and physics at the Institut National Polytechnique de Grenoble (INP), Grenoble, France. His research interests are in the modeling of nanoelectronic devices, 3-D simulations of quantum transport, and band-structure calculations.



John R. Barker graduated from the University of Edinburgh, Edinburgh, U.K., and the University of Durham, Durham, U.K., and received the Ph.D. degree in theoretical solid state physics from the University of Warwick, Coventry, U.K., in 1969, where he held a Personal SRC Fellowship.

From 1970 to 1985, he was a Lecturer, then Senior Lecturer, in theoretical physics with the University of Warwick. Since 1985, he has been Professor of Electronics in the Department of Electronics and Electrical Engineering, University of Glasgow, Glasgow, Scotland, U.K., where he was a Cofounder of the Nanoelectronics Research Centre with responsibility for the theory and modeling activities. He has been a Visiting Professor at Colorado State University, Fort Collins, and North Texas State University (now University of North Texas), Denton, and a Visiting Scientist with IBM T.J. Watson Laboratories, Yorktown Heights, NY. He has a broad range of research interests that currently include Green function modeling of nanodevices, silicon–germanium hetero-MOS, interface-roughness modeling, smart dust, and highly parallel computer architectures. He has over 300 publications in semiconductor physics, hot-electron theory, quantum-transport theory, Monte Carlo simulation, device physics and modeling, quantum theory of atomistic effects in ultrasmall devices, parallel computing, olfactory sensors, and molecular electronics.

Prof. Barker is a Fellow of the Royal Society of Edinburgh and Royal Astronomical Society.



Alexei Svizhenko received the B.S. and M.S. degrees from Moscow Institute of Physics and Technology, Moscow, Russia, in 1993 and 1995, respectively, and the Ph.D. degree in electrical engineering from the University of Nebraska, Lincoln, in 1999.

From 1999 to 2005, he was a Staff Scientist with Ames Center for Nanotechnology, National Aeronautics and Space Administration (NASA), Moffett Field, CA. In 2005 and 2006, he was a Research Scientist with Stanford University, Stanford, CA. Since 2006, he is with SILVACO International, Santa Clara, CA, as a Senior TCAD Engineer. His research interests are in the modeling and computation of quantum transport in nanotransistors, silicon nanowires, and carbon nanotubes.

Dr. Svizhenko was the recipient of the 2000 NASA Group Achievement Award and the 2003 and 2004 Computer Sciences Corporation Best Paper Award.

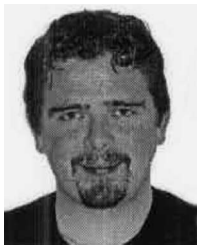


M. P. Anantram received the B.Sc. degree in applied sciences from the PSG College of Technology, Coimbatore, India, in 1986, the M.Sc. degree in physics from the University of Poona, Pune, India, in 1989, and the Ph.D. degree in electrical engineering from Purdue University, West Lafayette, Indiana, in 1995.

He was the Group Lead for Computational Nanoelectronics and, since 2004, a Fellow with the University Affiliated Research Center (UARC), National Aeronautics and Space Administration Ames Research Center, where his group developed the first 2-D quantum simulator for nanotransistors, and he codeveloped an algorithm to compute the charge and current density in nanodevices. He has also worked extensively on the modeling and prediction of electrical and electromechanical properties of nanostructures. Since May 2006, he has been a Professor with the Nanotechnology Engineering Group, Department of Electrical and Computer Engineering, University of Waterloo, Waterloo, ON, Canada. His research encompasses theory and computational modeling of semiconductor and molecular nanodevices.

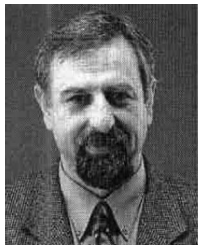
Dr. Anantram is an Associate Editor of the IEEE TRANSACTIONS IN NANOTECHNOLOGY and the Education Chair of the IEEE Nanotechnology Council. He serves on the program and organizing committees of nanotechnology conferences. He has received best paper awards for his work on nanotransistors and electromechanical properties of nanotubes. He coreceived the Computer Sciences Corporation's Highest Technical Achievement in Applied Sciences in 2003.

Authorized licensed use limited to: University of Washington Libraries. Downloaded on September 13,2024 at 22:03:16 UTC from IEEE Xplore. Restrictions apply.



Campbell Millar received the B.Eng. degree in electronics engineering with music in 1999 and the Ph.D. in 3-D simulation of bionanoelectronics from the University of Glasgow, Glasgow, U.K., in 2004.

From 2004 to 2006, he participated in the bionanotechnology IRC and developed advanced simulation codes for the simulation of charge transport in biological macromolecules. He is currently the Project Coordinator for the U.K. eScience Pilot Project "Meeting the design challenges of Nano-CMOS Electronics" in the Department of Electronics and Electrical Engineering, University of Glasgow. His research interests include parallel high-performance computing techniques and numerical algorithms, including multigrid methods, both continuum and particle simulation methodologies, advanced mesh-generation techniques, and the simulation of fluctuations in ultrasmall semiconductor devices.



Asen Asenov (M'96–SM'05) received the M.Sc. degree in solid state physics from Sofia University, Sofia, Bulgaria, in 1979 and the Ph.D. degree in physics from The Bulgarian Academy of Science, Sofia, in 1989.

He had ten years industrial experience as a Head of the Process and Device Modeling Group in IME-Sofia, developing one of the first integrated process and device CMOS simulators IMPEDANCE. From 1989 to 1991, he was a Visiting Professor with the Physics Department, TU Munich. Since 1991, he has been a member of the Department of Electronics and Electrical Engineering, University of Glasgow, Glasgow, Scotland, U.K., and served as the Head of the department from 1999 to 2003. As a Professor of device modeling, Leader of the Glasgow Device Modeling Group, and Academic Director of the Glasgow Process and Device Simulation Centre, he coordinates the development of 2-D and 3-D quantum–mechanical, Monte Carlo, and classical device simulators and their application in the design of advanced and novel CMOS devices. He has pioneered the simulations and the study of various sources of intrinsic parameter fluctuations in decanano- and nano-CMOS devices including random dopants, interface roughness, and line-edge roughness. He has over 330 publications in semiconductor-device physics on process and device modeling and simulation. He is an expert on atomistic effects in ultrasmall devices and impact of variations on circuits and systems including more than 15 papers in IEEE TRANSACTIONS ON ELECTRON DEVICES in the last five years. He has also given more than 65 invited talks at prestigious international conferences and meetings in Europe, USA, and Japan.

Prof. Asenov is a Fellow of the Royal Academy of Scotland and a member of the IEEE EDS TCAD Committee. He is currently a member of the Program committees for IEDM, ESSDERC, IWCE, SNW, HCIS, and IEEE Nano Conference and SNW2006.

Authorized licensed use limited to: University of Washington Libraries. Downloaded on September 13,2024 at 22:03:16 UTC from IEEE Xplore. Restrictions apply.